Scientific Research Publishing

Analysis of Effect of Oblateness of Smaller Primary on the Evolution of Periodic Orbits

Niraj Pathak[1], V. O. Thomas[2]

[1]Department of Mathematics, Dharmsinh Desai University, Nadiad, India
[2]Department of Mathematics, The Maharaja Sayajirao University of Baroda, Vadodara, India
Email: niraj23481@yahoo.com, votmsu@gmail.com

Abstract

Evolution of periodic orbits in Sun-Mars and Sun-Earth systems are analyzed using Poincare surface of section technique and the effects of oblateness of smaller primary on these orbits are considered. It is observed that oblateness of smaller primary has substantial effect on period, orbit's shape, size and their position in the phase space. Since these orbits can be used for the design of low energy transfer trajectories, so perturbations due to planetary oblateness has to be understood and should be taken care of during trajectory design. In this paper, detailed stability analysis of periodic orbit having three loops is given for $A_2 = 0.0001$.

1. Introduction

A low-energy transfer trajectory [1] is a trajectory in space that allows spacecraft to change the existing orbits using very small amount of fuel in comparison with Hohmann transfer orbit. To construct low-energy transfer trajectories, we require periodic orbits of spacecrafts around both primary bodies. Space agencies are trying to place telescopes into deep space like NASA's Terrestrial Planet Finder and ESA's Darwin project, to find Earth-like planets around other stars exhibiting life. In order to make space mission to explore different aspects of far away objects, it is required to determine special types of orbits that cannot be found by classical approaches.

However, it is to be noted that the classical approaches to spacecraft design are like Hohmann transfer for Apollo Moon landings and swing bys of outer planets for voyager. But these missions were costly in terms of fuel. A very high fuel requirement for

space missions may cause it infeasible. A new class of low energy trajectories has been introduced recently in which low fuel burn is required to control the trajectory from initial position to the targeted final position. A proper understanding of low-energy trajectory can be seen in [2].

The planar restricted three body problem (PRTBP) describes the motion of a body of negligible mass compared to two massive bodies, called primaries that are moving in circular orbits due to their mutual gravitational attraction. The two primaries could be the Sun and Earth, or the Sun and Mars, or any other pair of heavenly bodies that can produce considerable gravitational field. We take the total mass of the primaries normalized to 1. Mass of bigger primary is taken as $1 - \mu$ and that of smaller primary is μ. The two main bodies rotate in the plane in circular orbits counter clockwise about their common center of mass and with angular velocity which is also normalized to 1. The third body, the spacecraft, has an infinitesimal mass and is free to move in the plane. Generalization to the 3-dimensional problem is of course important, but many of the essential dynamics can be captured well with the planar model. [1] studied low energy transfer to the Moon. In this study, they considered four bodies Sun-Earth-Moon-Spacecraft as coupled three body systems, namely Sun-Earth-spacecraft and Earth-Moon-spacecraft. They constructed low energy transfer trajectories from the earth which executed ballistic capture at the Moon.

[3] is a fundamental book on the RTBP. Because of the non-linear nature of the equations of motion involved in the study of the system, analytical methods may not give illuminating insights into the solution. So, Poincare surface of section (PSS) is widely used for finding the orbits of the infinitesimal particle (spacecraft) and analyzing periodic, quasi periodic and chaotic orbits. Solar system dynamics by [4] provide a detailed analysis of periodic orbits using PSS technique.

As per Kolmogorov-Arnold-Moser (KAM) theory (Moser, 1966), a fixed point on the Poincare surface of section represents a periodic orbit in the rotating frame, and the closed curves around the point correspond to the quasi-periodic orbits. [5] analyzed the PSS for Earth-Moon system without considering any perturbation. [6] also had analysed Sun-Mars system by incorporating perturbations due to solar radiation. They have identified periodic, quasi-periodic solutions and chaotic regions from the PSS. Similar studies have been made by [7] for Saturn Titan system. [8] analyzed the family "f" orbits around smaller primary under RTBP for 14 systems under ideal conditions. [9] had studied Liapunov orbits in the photogravitational RTBP with oblates. In this paper they study periodic motion around collinear equilibrium points for two and three dimension. Using numerical analysis they studied the effect of solar radiation pressure and oblateness on location and stability. [10] studied periodic orbits of the Hill problem by considering solar radiation and oblateness as perturbing forces. [11] had studied equilibrium points and periodic orbits of planar restricted three-body problem when both primaries are tri axial rigid bodies. [12] analyzed Periodic orbits generated by Lagrangian solutions of the restricted three body problem when one of the primaries is an oblate body. [13] studied Periodic orbits in the photogravitational restricted problem with

the smaller primary an oblate body. [14] computed series of horizontally critical symmetric periodic orbits of the six basic families of the restricted three-body problem when the more massive primary is an oblate spheroid. The vertical stability of the horizontally critical orbits is also computed.

A large number of periodic orbits were generated by [15] in the framework of RTBP numerically. He classified the orbits into ten families. His work widely referred in literature. These studies explore the regions of the phase space that contain sensitive dependence on initial conditions. [16] [17] and [18] made extensive study on phase space by exploring large portion of the phase plane with Poincare surfaces of section (PSS) [19]. This technique was also used by [20] [21] [22] and [23] to explore the phase space of a system with the Sun-Jupiter mass ratio.

Recently, [24] analyzed Sun and Saturn centered periodic orbits with solar radiation pressure and oblateness and found that there is a substantial effect of solar radiation pressure on position and geometry of infinitesimal particle orbit. [25] had studied family "*f*" orbits and their stability for Sun-Saturn system with perturbation. In their study Sun was taken as a source of radiation and Saturn was considered as oblate spheroid. By taking the actual coefficient of oblateness for Saturn and different values of solar radiation pressure, the family "*f*" orbits have been analyzed in detail.

Periodic orbits of spacecraft around two primaries are used to construct low energy trajectory. [26] established three classes with orbits around both primaries depending on motion of spacecraft is prograde or retrograde in the rotating system as well as fixed system. In this paper we have analyzed periodic orbits around both primaries with retrograde motion in rotating system and analyzed periodic orbits having number of loops from 1 to 5 for different pairs of oblateness coefficient A_2 and Jacobi constant C for Sun-Mars and Sun-Earth system. It has been found that A_2 and C has substantial effect on the position in phase space, shape and size of the orbits and hence must be considered during low energy trajectory design.

2. Equations of Motion

Let m_1 and m_2 be two masses of first primary and second primary bodies. Mass of first primary is greater than mass of second primary. The perturbed mean motion n of second primary body is given by,

$$n^2 = 1 + \frac{3}{2} A_2,$$

(1)

where

$$A_2 = \frac{\rho_e^2 - \rho_p^2}{5R^2}.$$

(2)

Here A_2 is oblateness coefficient of second primary. ρ_e and ρ_p represent equatorial and polar radii of second primary and R is the distance between two primaries. The unit of mass is chosen equal to the sum of the primary masses and the unit of length is equal to their separation. The unit of time is such that the Gaussian constant of gravitation is unity in the unperturbed case. The usual dimensionless synodic coordinate sys-

tem Oxy is used to express the motion.

Choose a rotating coordinate system with origin at the center of mass, the primaries lie on the x-axis at the points $(-\mu, 0)$ and $(1 - \mu, 0)$, respectively, where mass factor $\mu = \dfrac{m_2}{(m_1 + m_2)}$. Following [27], the equations of motion of the spacecraft are

$$\ddot{x} - 2n\dot{y} = \frac{\partial \Omega}{\partial x}, \quad \ddot{y} + 2n\dot{x} = \frac{\partial \Omega}{\partial y}, \tag{3}$$

where

$$\Omega = \frac{n^2}{2}\left[(1-\mu)r_1^2 + \mu r_2^2\right] + \frac{(1-\mu)}{r_1} + \frac{\mu}{r_2} + \frac{\mu A_2}{2r_2^3}. \tag{4}$$

Here

$$r_1^2 = (x - \mu)^2 + y^2, \tag{5}$$

and

$$r_2^2 = (x + 1 - \mu)^2 + y^2. \tag{6}$$

Equations (3) and (4) lead to the first integral

$$\dot{x}^2 + \dot{y}^2 = 2\Omega - C, \tag{7}$$

where C is Jacobi constant of integration given by

$$C = n^2\left((1-\mu)r_1^2 + \mu r_2^2\right) + 2\frac{(1-\mu)}{r_1} + 2\frac{\mu}{r_2} + \frac{\mu A_2}{r_2^3} - \dot{y}^2. \tag{8}$$

These equations of motion are integrated in (x, y) variables using a Runge-Kutta Gill fourth order variable or fixed step-size integrator. The initial conditions are selected along the x-axis. By defining a plane, say $y = 0$, in the resulting three dimensional space the values of x and $\dot{x}$ can be plotted every time the particle has $y = 0$, whenever the trajectory intersects the plane in a particular direction, say $\dot{y} > 0$. We have constructed Poincare surface section (PSS) on the x, $\dot{x}$ plane. The initial values were selected along the Ox-axis by using intervals of length 0.001. By giving different value of C we can plot the trajectories, and then analysis of orbits can be done.

3. Results and Discussion

We shall consider two systems, the Sun-Mars system and the Sun-Earth system. The mass of Sun, Earth and Mars considered in the study are 1.9881×10^{30} kg, 5.972×10^{24} kg and 6.4185×10^{23} kg, respectively, [5]. Thus, for the Sun-Earth and Sun-Mars systems, mass factor μ are 0.000003002 and 0.0000003212 respectively. Equatorial and polar radii of Earth are 6378.1 kms. and 6356.8 kms. and that of Mars are 3396.2 kms. and 3376.2 kms., respectively. The distance between Sun and Earth is taken as 149,600,000 kms. and distance between Sun and Mars is 227,940,000 kms. So, oblateness coefficient calculated from Equation (2) for Sun-Earth and Sun-Mars have values $A_2 = 2.42405 \times 10^{-12}$ and $A_2 = 5.21389 \times 10^{-13}$ respectively. Though these values of oblateness are neg-

ligible, they definitely affect orbits with close proximity. In order to study the effect of oblateness on periodic orbit around both primaries, we take different values of oblateness that can make observable changes in different parameters. For a given A_2, selection of C is not arbitrary. By solving Equation (8) w.r.t. $\dot{x}^2$ and by setting in to this equation $y = 0$ and $\dot{y}^2 > 0$ the resulting inequality defines the regions allowed to motion on the PSSs. Thus, we eliminate the possibility of excluded region for secondary body between Sun and Earth (or Mars). This maximum value of C is considered as admissible value of C.

Table 1 and Table 2 show range of admissible values of C for Sun-Mars and Sun-Earth systems. It can be observed that for both systems as oblateness increases, admissible range of C increases. But this increment is larger for Sun-Earth system than Sun-Mars system. So, we can say that as mass factor increases, effect of oblateness increases and due to that admissible range of C increases.

We have studied the effect of oblateness on the location and period of Sun-Mars system for different values of Jacobi constant C using PSS. Figure 1 is PSS constructed for Sun-Mars system when (A_2, C) is (0.0005, 2.93) by taking value of x from the interval [0.8, 1] with interval of x differencing as 0.001. Also, time span $t = 10,000$ time units and interval of time differencing is taken as 0.001. So, for each x equations of motions are integrated using Runge-Kutta-Gill method. Each solution is plotted as a point in Figure 1. The arcs of PSS are known as islands whose center gives periodic orbit.

In a similar way, we can obtain PSS for Sun-Earth which is shown in Figure 2. This PSS is also constructed for the pair (A_2, C) given by (0.0005, 2.93). Our aim is to make a comparative study of the effect of oblateness on different parameters of the orbits of Sun-Earth and Sun-Mars systems using PSS technique. Mass factor μ of Sun-Earth is greater than Sun-Mars.

For Sun-Mars system, the numerical values of location of periodic orbit and left end

**Table 1.** Admissible range of C for Sun-Mars system.

A_2	Maximum value of C	Value of C greater than maximum value	Excluded region (where $\dot{y}$ is complex)	Size of excluded region
0.00001	3.00	3.001	0.984 to 0.999	0.016
0.00005	3.00	3.001	0.984 to 0.998	0.015
0.0001	3.00	3.001	0.985 to 0.997	0.013
0.0005	3.001	3.002	0.981 to 0.995	0.015

Table 2. Admissible range of C for Sun-Earth system.

A_2	Maximum value of C	Value of C greater than maximum value	Excluded region (where $\dot{y}$ is complex)	Size of excluded region
0.00001	3.00	3.001	0.988 to 0.992	0.005
0.00005	3.001	3.002	0.978 to 0.995	0.018
0.0001	3.001	3.002	0.979 to 0.993	0.015
0.0005	3.002	3.003	0.976 to 0.990	0.015
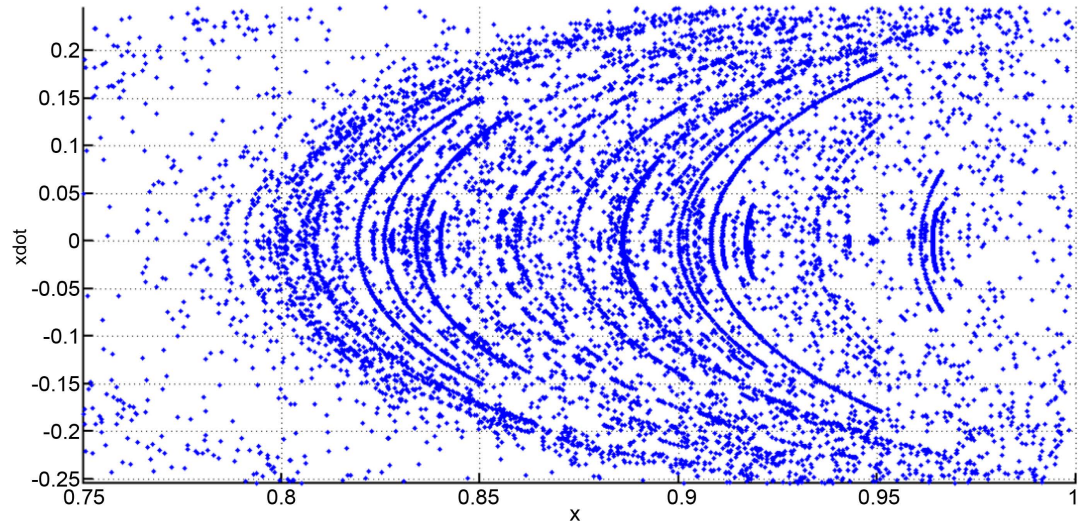
Figure 1. PSS for $A_2 = 0.0005$ and $C = 2.93$, for $x = [0.8, 1]$, $t = 10,000$ for Sun-Mars system.
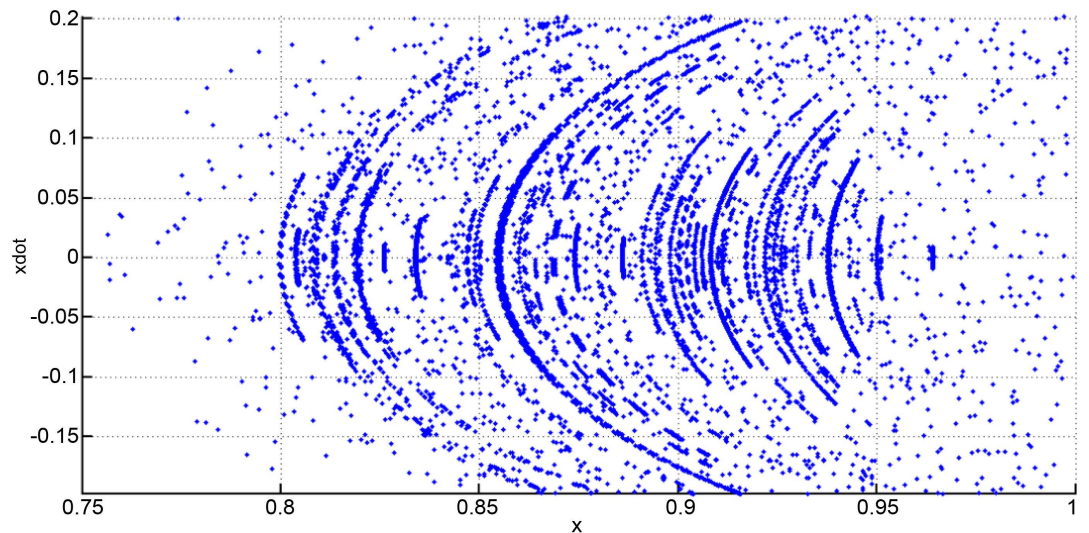
Figure 2. PSS for $A_2 = 0.0005$ and $C = 2.93$, for $x = [0.8, 1]$, $t = 10,000$ for Sun-Earth system.

(L) and right end (R) of corresponding island for $C = 2.93$, 2.94, 2.95, 2.96 and for oblateness $A_2 = 0.00001$, 0.00005, 0.0001 and 0.0005 are displayed in **Table 3**. It is observed from the table that a change in C in the range (2.93, 2.96) affects the location of the periodic orbits. Oblateness also affects the location of the periodic orbit. Similarly, the effects of C and A_2 in the location of periodic orbits and left end (L) and right end (R) of corresponding island for the Sun-Earth system are studied and the numerical estimates of the changes are displayed in **Table 4**. Size of the island gives stability of the corresponding orbit.

The periodic orbits starting from single-loop to five loops in the Sun-Mars and Sun-Earth systems for $A_2 = 0.0005$ and $C = 2.93$ are shown in **Figures 3(a)-(j)**. It can be observed, from **Figure 3** that the width of the orbit decreases continuously as the number of loops increases. Further in all cases the infinitesimal particle (spacecraft) orbits

Table 3. Analysis of periodic orbit for different pairs of A_2 and C for Sun-Mars system.

NO. OF LOOPS	C	$A_2 = 0.00001$			$A_2 = 0.00005$			$A_2 = 0.0001$			$A_2 = 0.0005$		
		Location (x)	L	R	Location (x)	L	R	Location (x)	L	R	Location (x)	L	R
1	2.96	0.98295	0.9829	0.983	0.98285	0.9827	0.983	0.98272	0.9825	0.9829	0.9816	0.9815	0.9817
	2.95	0.9679	0.9678	0.968	0.9678	0.9676	0.968	0.96765	0.9669	0.9686	0.9666	0.966	0.967
	2.94	0.95324	0.953	0.9535	0.95314	0.953	0.9533	0.953	0.953	0.953	0.95196	0.9519	0.952
	2.93	0.93896	0.9389	0.939	0.93887	0.9387	0.939	0.93875	0.9386	0.9389	0.93772	0.9376	0.9378
2	2.96	0.94149	0.9406	0.9425	0.94136	0.9411	0.9414	0.94119	0.941	0.9414	0.93985	0.9397	0.94
	2.95	0.92251	0.9224	0.9226	0.92239	0.9223	0.9225	0.92223	0.922	0.9225	0.92096	0.9209	0.921
	2.94	0.9045	0.9042	0.905	0.90438	0.9041	0.905	0.90424	0.904	0.9045	0.90302	0.903	0.903
	2.93	0.88734	0.887	0.8878	0.88722	0.887	0.8874	0.88708	0.887	0.8872	0.88592	0.8858	0.886
3	2.96	0.91529	0.915	0.9156	0.91514	0.915	0.9153	0.91496	0.9149	0.915	0.91348	0.9133	0.9137
	2.95	0.89425	0.894	0.8945	0.89412	0.894	0.8942	0.89395	0.8939	0.894	0.89258	0.8922	0.893
	2.94	0.87463	0.8743	0.8748	0.87449	0.8743	0.8747	0.87433	0.874	0.8747	0.87305	0.873	0.8731
	2.93	0.85616	0.856	0.8563	0.85604	0.856	0.8561	0.85588	0.8558	0.856	0.85467	0.8543	0.855
4	2.96	0.89703	0.897	0.8971	0.89688	0.8968	0.897	0.89668	0.8965	0.8969	0.89515	0.895	0.8953
	2.95	0.8749	0.8748	0.875	0.87476	0.8745	0.875	0.87458	0.874	0.875	0.87316	0.873	0.8733
	2.94	0.85447	0.8544	0.8545	0.85433	0.854	0.8547	0.85417	0.8541	0.8543	0.85284	0.8527	0.853
	2.93	0.8354	0.835	0.836	0.83528	0.835	0.8357	0.83512	0.835	0.8353	0.83388	0.8338	0.834
5	2.96	0.88363	0.8832	0.8834	0.88347	0.883	0.8838	0.88328	0.883	0.8836	0.8817	0.8814	0.882
	2.95	0.8609	0.8608	0.861	0.86075	0.8605	0.861	0.86057	0.8602	0.8609	0.85912	0.859	0.8593
	2.94	0.84004	0.84	0.8401	0.83991	0.8398	0.84	0.83974	0.8394	0.8401	0.83839	0.8383	0.8385
	2.93	0.82068	0.8204	0.821	0.82056	0.8205	0.8206	0.8204	0.82	0.8208	0.81914	0.819	0.8193

Table 4. Analysis of periodic orbit for different pairs of A_2 and C for Sun-Earth system.

| NO. OF LOOPS	C	$A_2 = 0.00001$			$A_2 = 0.00005$			$A_2 = 0.0001$			$A_2 = 0.0005$		
		Location (x)	L	R	Location (x)	L	R	Location (x)	L	R	Location (x)	L	R
1	2.96	0.983	0.983	0.983	0.9829	0.9828	0.983	0.9828	0.9828	0.9828	0.9817	0.9817	0.9817
	2.95	0.9679	0.9678	0.968	0.96782	0.9676	0.968	0.9677	0.9674	0.968	0.9666	0.9662	0.967
	2.94	0.95325	0.953	0.9535	0.95315	0.953	0.9533	0.95304	0.9530	0.9531	0.952	0.952	0.952
	2.93	0.939	0.939	0.939	0.9389	0.9388	0.939	0.93877	0.9385	0.939	0.93775	0.9375	0.938
2	2.96	0.94155	0.941	0.942	0.9414	0.941	0.9418	0.94125	0.941	0.9415	0.9399	0.9398	0.94
	2.95	0.92255	0.9221	0.923	0.92244	0.922	0.923	0.92226	0.922	0.9225	0.921	0.921	0.921
	2.94	0.90455	0.904	0.9051	0.90442	0.904	0.9048	0.90426	0.904	0.9045	0.90305	0.903	0.9031
	2.93	0.88737	0.887	0.8877	0.88725	0.887	0.8875	0.8871	0.887	0.8872	0.88595	0.8859	0.886
3	2.96	0.91535	0.915	0.9157	0.9152	0.915	0.9154	0.915	0.915	0.915	0.91354	0.9131	0.9141
	2.95	0.8943	0.894	0.8946	0.89416	0.894	0.8943	0.894	0.894	0.894	0.89262	0.8922	0.893
	2.94	0.87465	0.8743	0.875	0.87453	0.8741	0.875	0.87438	0.874	0.8748	0.87309	0.873	0.8732
	2.93	0.8562	0.8554	0.857	0.85608	0.856	0.8562	0.85592	0.8558	0.856	0.8547	0.8544	0.855
4	2.96	0.8971	0.897	0.8972	0.89695	0.8969	0.897	0.89675	0.8965	0.897	0.8952	0.895	0.8954
	2.95	0.87495	0.8749	0.875	0.87482	0.8746	0.875	0.87464	0.8743	0.875	0.87321	0.873	0.8734
	2.94	0.8545	0.854	0.855	0.85438	0.854	0.8548	0.85421	0.854	0.8544	0.85289	0.8528	0.853
	2.93	0.83544	0.835	0.8359	0.83532	0.835	0.8356	0.83516	0.835	0.8353	0.83392	0.8338	0.834
5	2.96	0.8837	0.8834	0.884	0.88353	0.883	0.8841	0.88334	0.883	0.8837	0.88175	0.8815	0.882
	2.95	0.86095	0.8609	0.861	0.8608	0.8606	0.861	0.86062	0.8602	0.861	0.85918	0.859	0.8594
	2.94	0.8401	0.84	0.8402	0.83995	0.8399	0.84	0.83978	0.8396	0.84	0.83844	0.838	0.8389
	2.93	0.82072	0.8204	0.821	0.8206	0.82	0.821	0.82044	0.82	0.8209	0.81918	0.819	0.8194
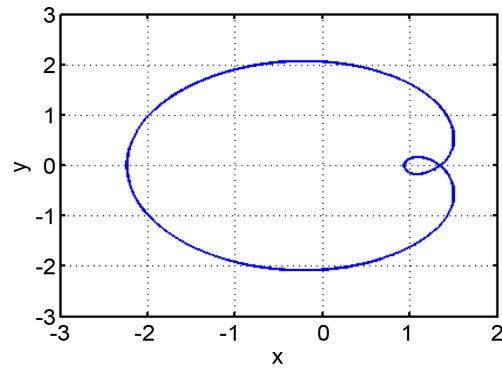
(a) Sun-Mars system $C = 2.93$, $A_2 = 0.0005$, period 13.
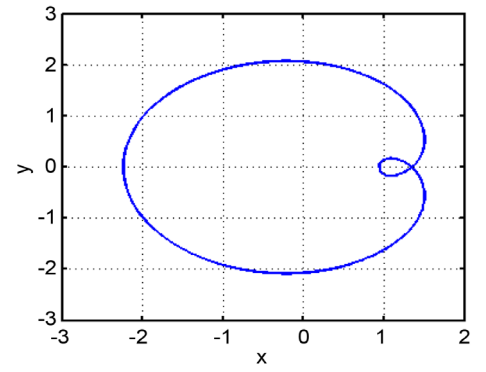
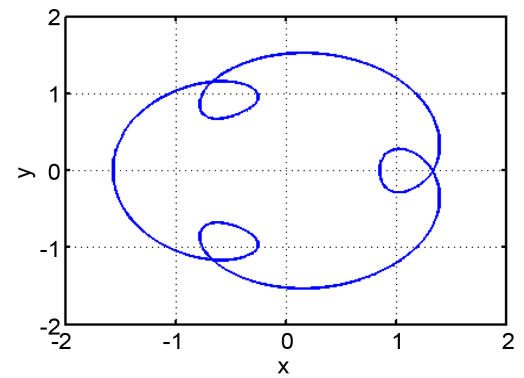(b) Sun-Earth system $C = 2.93$, $A_2 = 0.0005$, period 13.
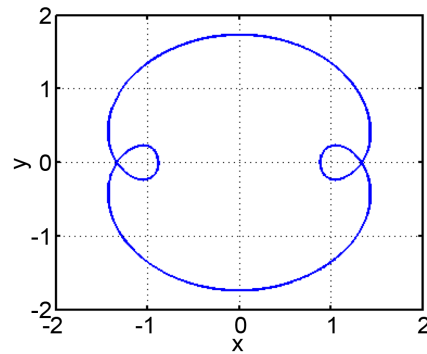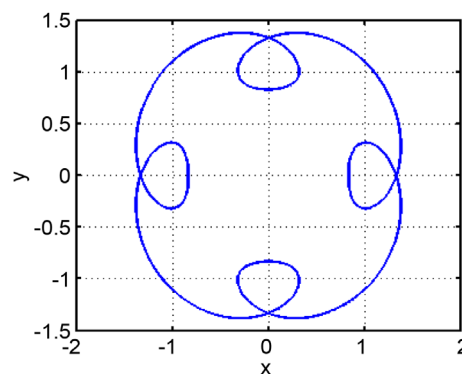
(c) Sun-Mars system $C = 2.93$, $A_2 = 0.0005$, period 19.
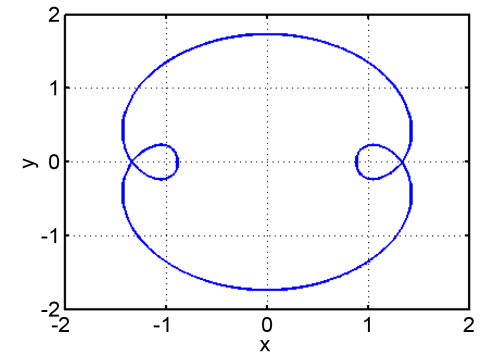
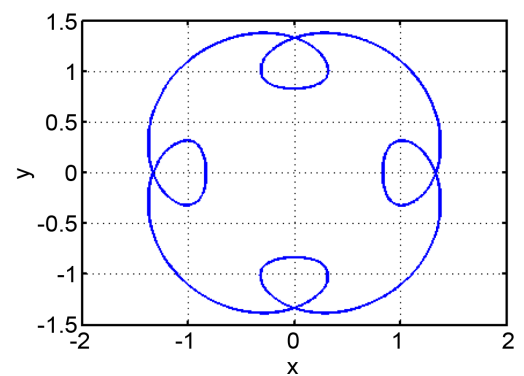(d) Sun-Earth system $C = 2.93$, $A_2 = 0.0005$, period 19.
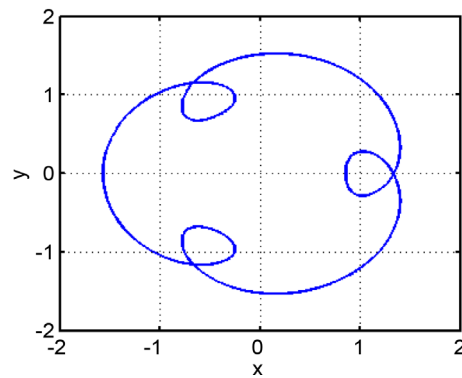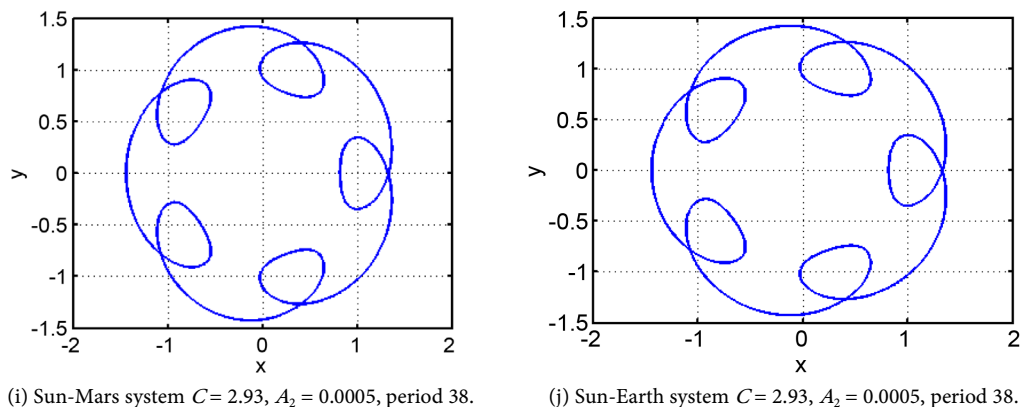
(e) Sun-Mars system $C = 2.93$, $A_2 = 0.0005$, period 26.

(f) Sun-Earth system $C = 2.93$, $A_2 = 0.0005$, period 26.

(g) Sun-Mars system $C = 2.93$, $A_2 = 0.0005$, period 32.

(h) Sun-Earth system $C = 2.93$, $A_2 = 0.0005$, period 32.

(i) Sun-Mars system $C = 2.93$, $A_2 = 0.0005$, period 38.   (j) Sun-Earth system $C = 2.93$, $A_2 = 0.0005$, period 38.

Figure 3. Periodic orbits around both primaries for Sun-Mars and Sun-Earth systems.

around the second primary (Mars or Earth) in addition to orbiting both primaries. Further the secondary body is closest to Mars or Earth in the single-loop closed orbit. Such orbits may be useful in the study of different aspects of both primaries. In many models available in literature not many closed orbits possess this kind of nature. Further the position of the orbit in the case of odd number of loops approaches the first primary, namely the Sun. This is true in the case of even number of loops also. It can be observed that the period of the orbit remains unchanged due to change in oblateness or mass factor, but period of the orbit increases with increment in number of loops.

We have studied the variation of position of periodic orbits around Sun-Mars and Sun-Earth system due to the variation in oblateness and Jacobi constants C. In **Figure 4** we have shown the variation of position of closed periodic orbit with single-loop for oblateness in the range (0, 0.0005) for Sun-Mars system corresponding to Jacobi constants $C = 2.93$, 2.94, 2.95 and 2.96. From **Figure 5** it is clear that the position of the orbits recedes away from Mars when the oblateness increases and C decreases.

Similar kind of conclusion can be drawn from **Figure 5** for the Sun-Earth system.

We have studied the effect of A_2 and C on the position of the orbits having loops varying from 1 to 5 for both Sun-Mars and Sun-Earth systems. The results of these observations for 5 loops closed periodic orbit in both Sun-Mars and Sun-Earth systems are shown in **Figure 6** and **Figure 7**.

From **Figure 8** and **Figure 9**, it can be observed that for given oblateness, location of periodic orbit moves away from second primary as number of loops in periodic orbit increase. Also, as oblateness increases, location of periodic orbit moves away from second primary.

We have analyzed stability of periodic orbits from loop 1 to 5 for $A_2 = 0.00001$, 0.00005, 0.0001 and 0.0005. Since stability behavior is similar for all these orbits, in this paper stability analysis for three loops orbit corresponding to $A_2 = 0.0001$ is given. **Figure 10** shows stability region for $A_2 = 0.0001$ for three loop orbits. The left and right tips of the island are plotted by red and green curves, respectively. From **Figure 10** it is clear that size of stability region is very small in comparison to "f" family orbit [9]. So, these periodic orbits can be used as a transfer orbits as they are not stable. So, secondary
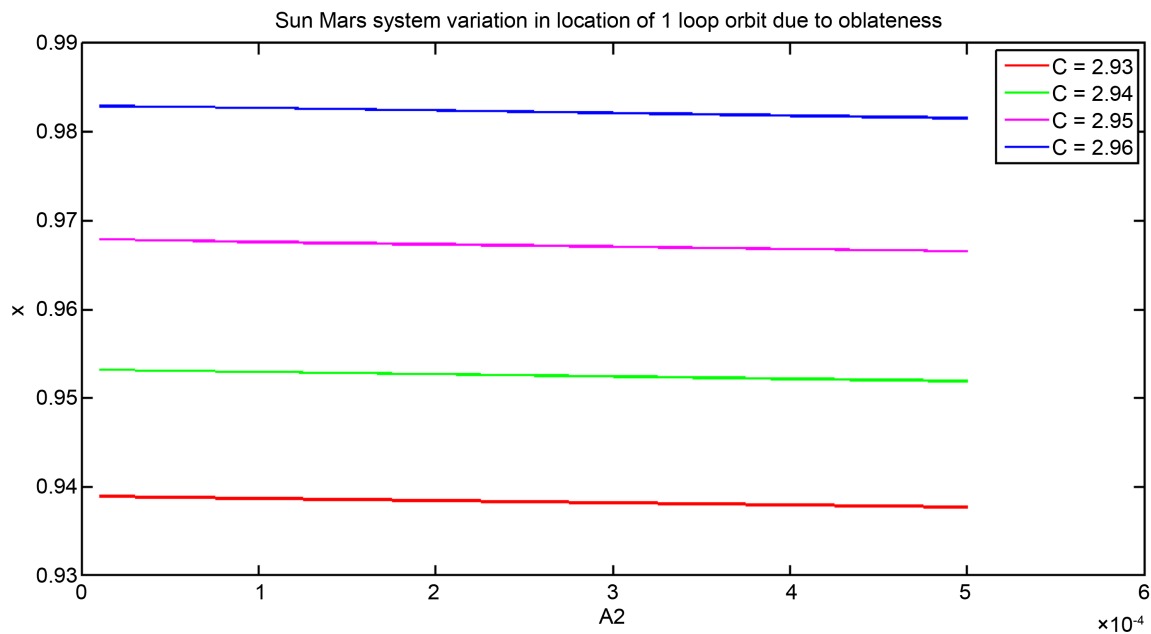
Sun Mars system variation in location of 1 loop orbit due to oblateness

Figure 4. Variation in location of single-loop periodic orbit around Sun-Mars system due to oblateness.

Sun Earth system variation in location of 1 loop orbit due to oblateness
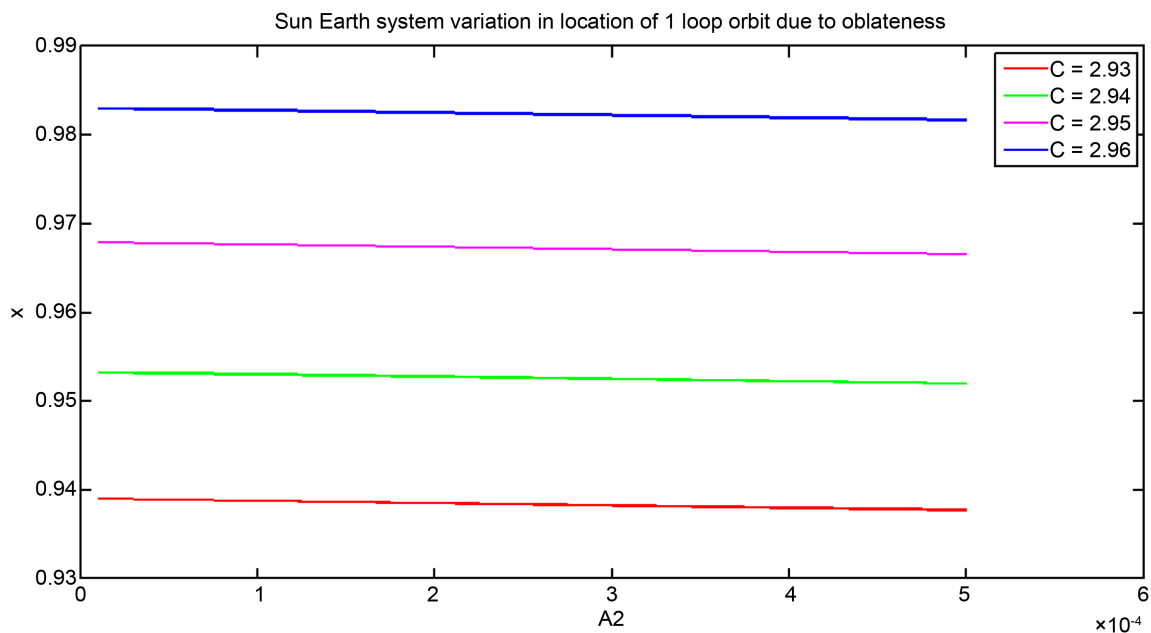

Figure 5. Variation in location of single-loop periodic orbit around Sun-Earth due to oblateness.

body required few amount of fuel than Hohmann transfer. **Figure 11** shows amplitude for three loops orbit when $A_2 = 0.0001$. It can be observe that there are two separatrices at $C = 2.95$ and 2.96 where stability of the periodic orbit is zero as the size of the island is zero. For $C = 2.94$ we get maximum stability which is 0.0008. **Figure 12** shows size of the island for $C = 2.94$ for three loops orbit when $A_2 = 0.0001$ which is 0.0008 whereas **Figure 13** shows PSS of first separatrix at $C = 2.95$ which is looks like a straight line where as for "f" family orbit it is triangular due to third order resonance [9]. It can be
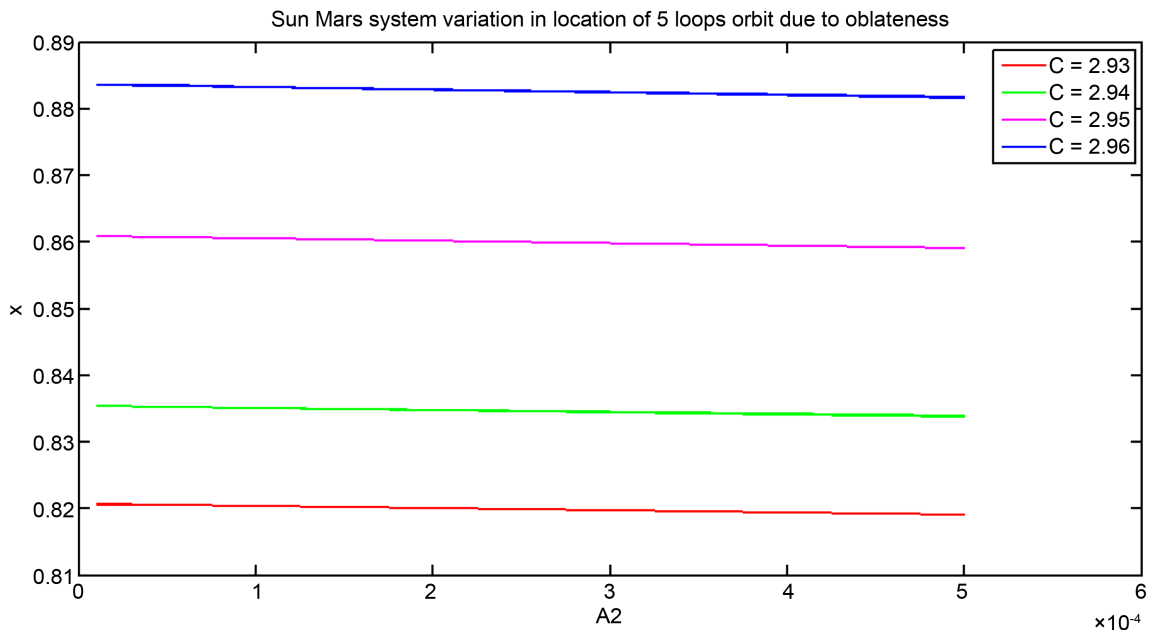
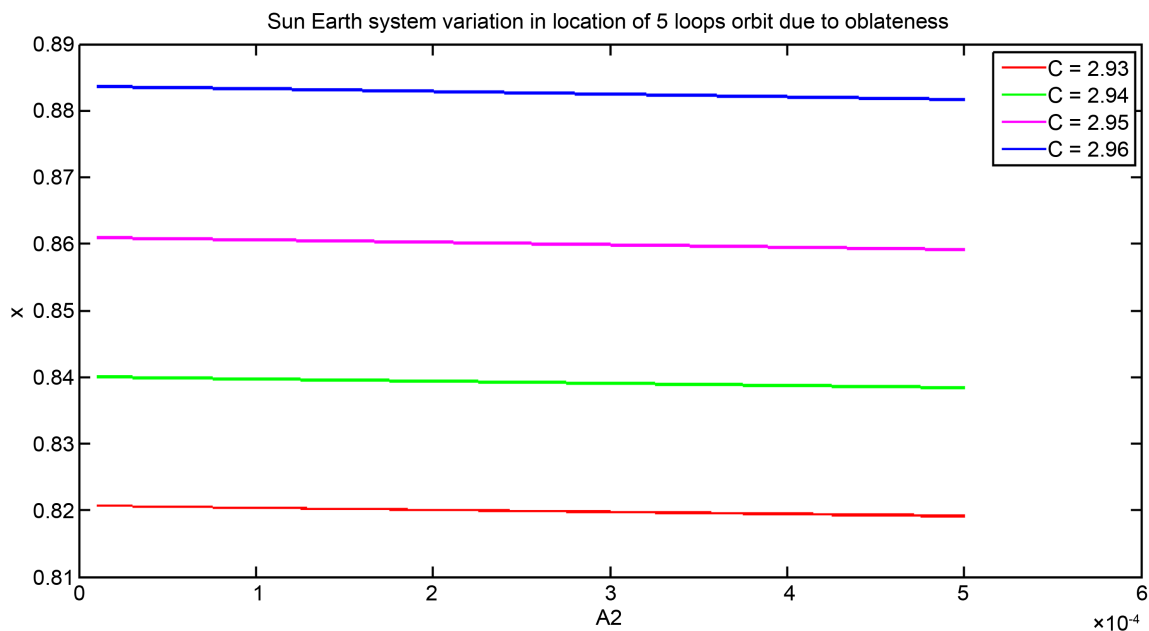**Figure 6.** Variation in location of five loops periodic orbit around Sun-Mars system due to oblateness.

Figure 7. Variation in location of five loops periodic orbit around Sun-Earth system due to oblateness.

seen that size of this island is zero. **Figure 14** shows three loops orbit corresponding to first separatrix when $A_2 = 0.0001$. **Figure 15** shows for $C = 2.955$ again size of island increases and it becomes 0.0006, where as for $C = 2.96$ again size of island becomes zero, which is second separatrix as shown in **Figure 16**. Three loops orbit corresponding to second separatrix is given in **Figure 17**.

In **Table 5** initial velocity of secondary body is denoted by V, D_1 and D_2 are the distance of secondary body from Mars and Sun respectively. V is in kms^{-1}, D_1 and D_2 are
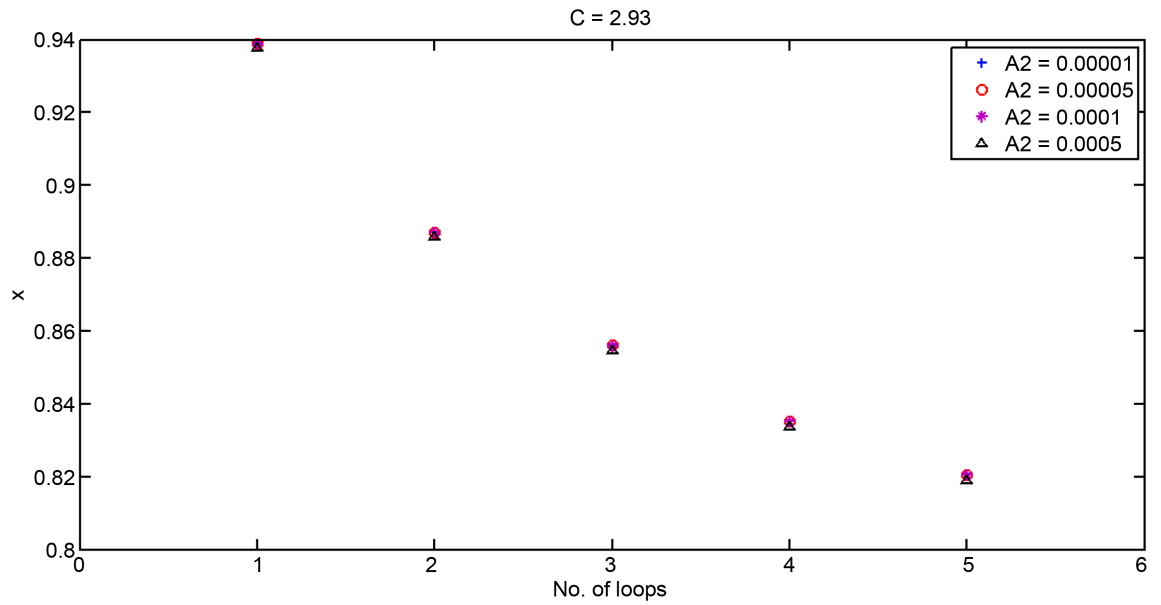
Figure 8. Variation in location of periodic orbit of secondary body around Sun and Mars for $C = 2.93$ due to number of loops for different oblateness A_2.
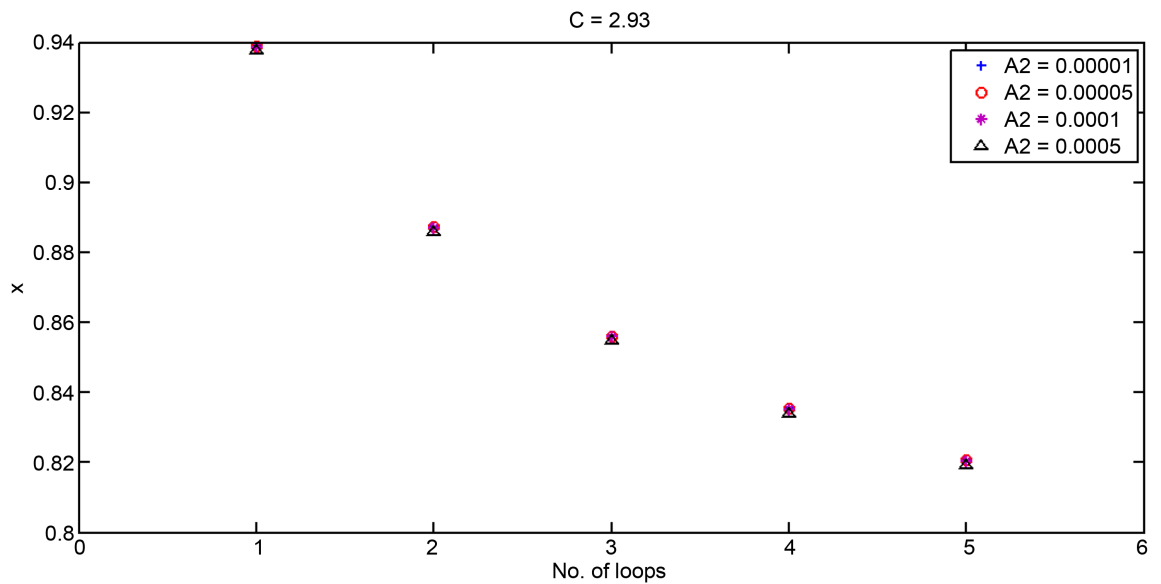
Figure 9. Variation in location of periodic orbit of secondary body around Sun-Earth system for $C = 2.93$ due to number of loops for different oblateness A_2.

in km. Similar notations are used in **Table 6** also. In **Table 6** distance of secondary body from Earth is denoted by D_1.

$$V^2 = \left(\dot{x}^2 + \left(\dot{y} + x + \mu \right)^2 \right), \tag{9}$$

V can be obtained using Equation (9).

The conversion from units of distance (I) and velocity (J) in the normalized dimensionless system to the dimensionalized system is given by,
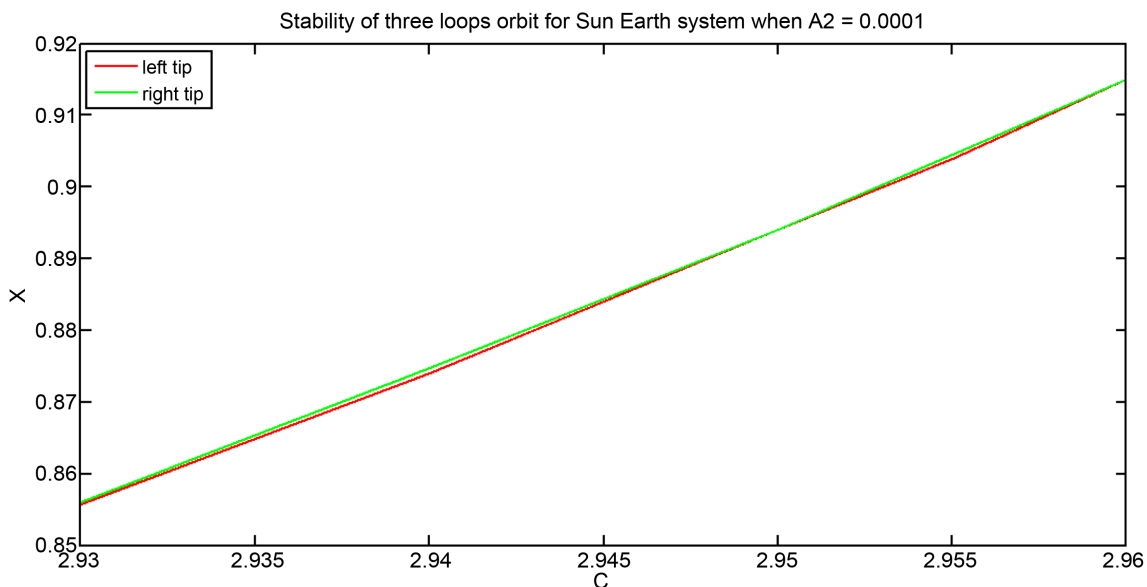
Figure 10. Stability analysis for three loops orbit for Sun-Earth system when $A_2 = 0.0001$.
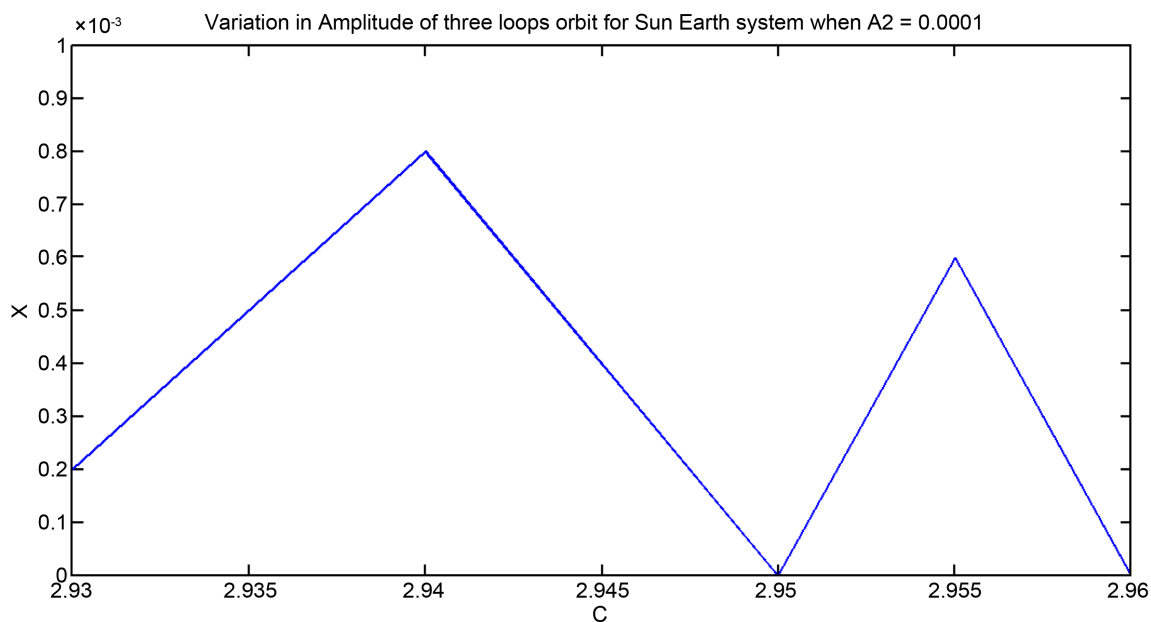
Figure 11. Amplitude for three loops orbit for Sun-Earth system when $A_2 = 0.0001$.

$$\text{Distance} \quad D = L \times I \tag{10}$$

$$\text{Velocity} \quad V = O \times J \tag{11}$$

where L is the distance between the centers of both primaries in km. O is the orbital velocity of second primary around first primary [2]. For Sun-Mars and Sun-Earth system $L = 227,940,000$ and $149,600,000$ km respectively. Mean orbital velocity of Mars around Sun and Earth around Sun are 24.07 km·sec^{-1} and 29.78 km·sec^{-1} respectively.

It can be observed from **Table 5** and **Table 6** that for given oblateness and given loop orbit as C decreases, V and D_1 increase while D_2 decreases. For a given C and given
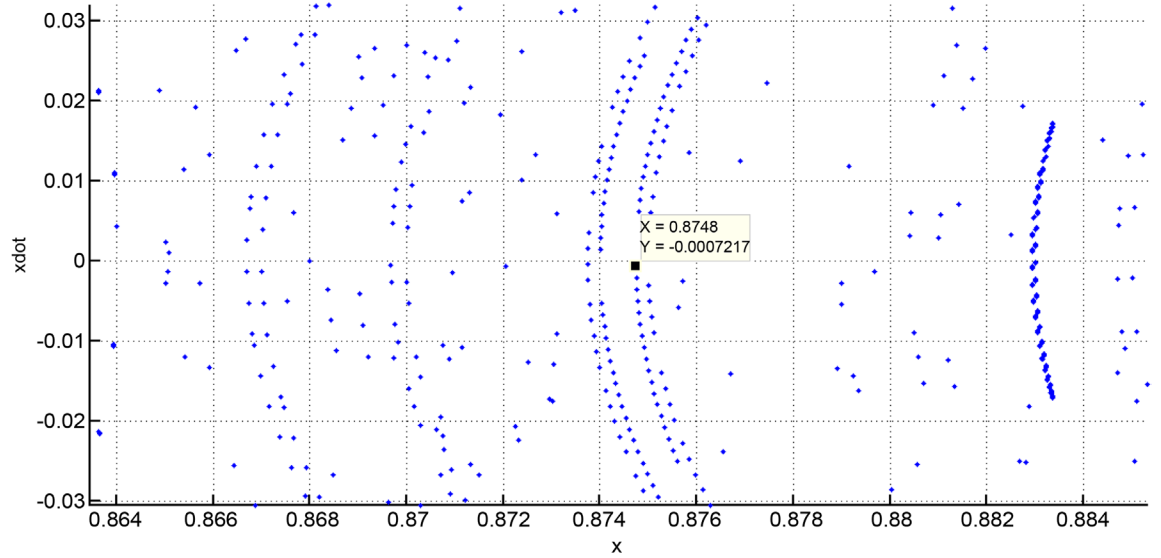
Figure 12. Enlarge view of PSS for $C = 2.94$ when $A_2 = 0.0001$.
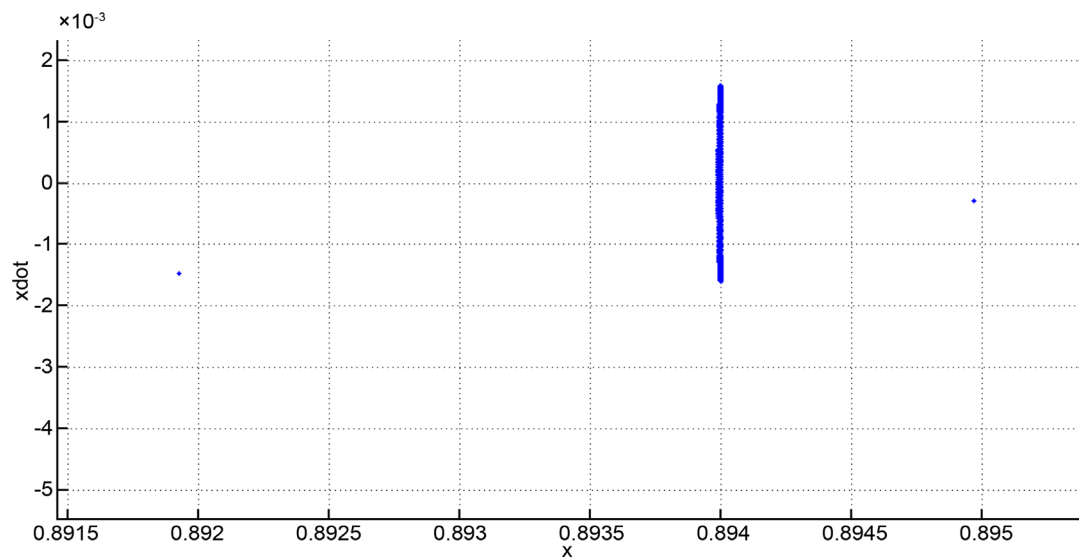
Figure 13. Enlarge view of PSS of first separatrix for two loops orbit for $C = 2.95$ when $A_2 = 0.0001$.
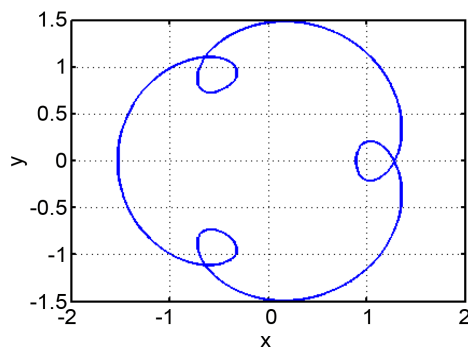
Figure 14. Orbit at first separatrix corresponding to $C = 2.95$, $A_2 = 0.0001$ and $x = 0.894$.

Figure 15. Enlarge view of PSS for $C = 2.955$ when $A_2 = 0.0001$.

Figure 16. Enlarge view of PSS of second separatrix for three loops orbit for $C = 2.96$ when $A_2 = 0.0001$.

Figure 17. Orbit at second separatrix corresponding to $C = 2.96$, $A_2 = 0.0001$, and $x = 0.915$.

Table 5. Location, velocity and distance of orbit from both primaries for A_2 = 0.00001, 0.00005, 0.0001, 0.0005 for Sun-Mars system.

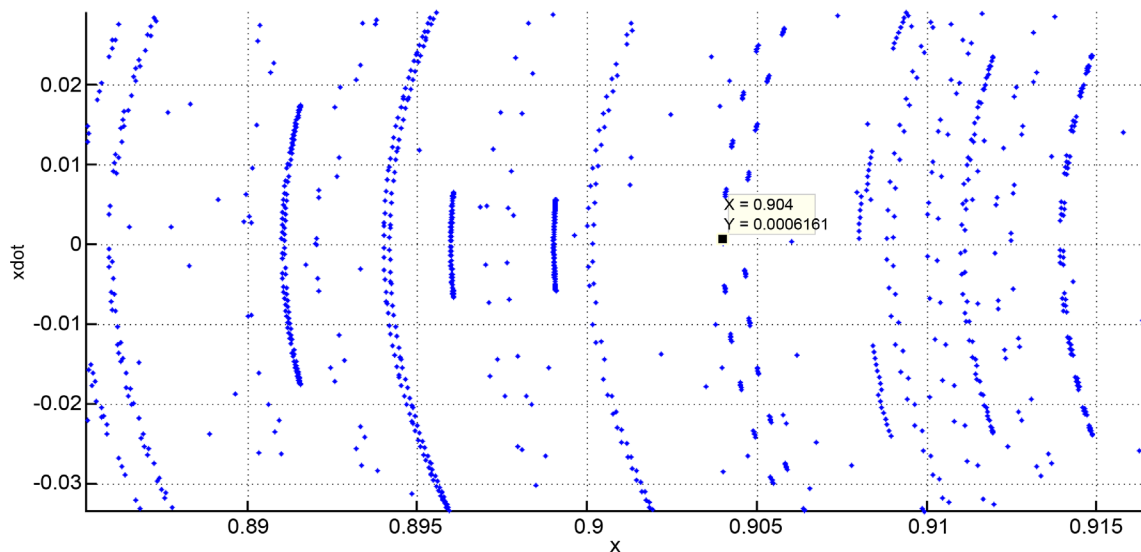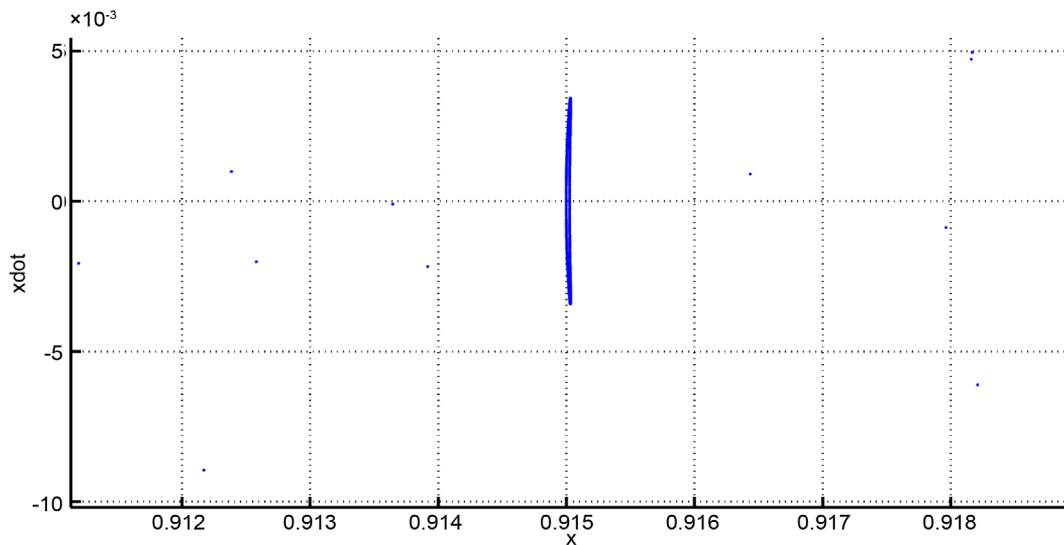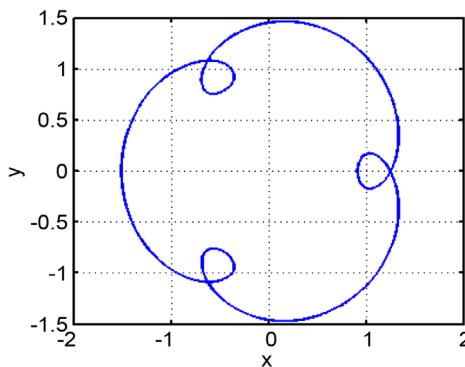| No. of loop	C	x	V (km·sec⁻¹)	D₁ (10⁷ km)	D₂ (10⁸ km)	x	V (km·sec⁻¹)	D₁ (10⁷ km)	D₂ (10⁸ km)	x	V (km·sec⁻¹)	D₁ (10⁷ km)	D₂ (10⁸ km)	x	V (km·sec⁻¹)	D₁ (10⁷ km)	D₂ (10⁸ km)
			A_2 = 0.00001				A_2 = 0.00005				A_2 = 0.0001				A_2 = 0.0005		
1	2.96	0.98295	28.52	0.3886	2.2405	0.98285	28.53	0.3909	2.2403	0.98272	28.53	0.3938	2.2400	0.9816	28.54	0.4194	2.2374
	2.95	0.9679	28.84	0.7316	2.2062	0.9678	28.85	0.7339	2.2060	0.96765	28.85	0.7373	2.2056	0.9666	28.86	0.7613	2.2032
	2.94	0.95324	29.16	1.0658	2.1728	0.95314	29.16	1.0681	2.1725	0.953	29.16	1.0713	2.1722	0.95196	29.18	1.0950	2.1698
	2.93	0.93896	29.48	1.3913	2.1402	0.93887	29.48	1.3933	2.1400	0.93875	29.48	1.3961	2.1397	0.93772	29.49	1.4196	2.1374
2	2.96	0.94149	28.08	1.3336	2.1460	0.94136	28.08	1.3366	2.1457	0.94119	28.08	1.3405	2.1453	0.93985	28.11	1.3710	2.1422
	2.95	0.92251	28.52	1.7662	2.1027	0.92239	28.53	1.7690	2.1024	0.92223	28.53	1.7726	2.1021	0.92096	28.55	1.8016	2.0992
	2.94	0.9045	28.96	2.1768	2.0617	0.90438	28.96	2.1795	2.0614	0.90424	28.96	2.1827	2.0611	0.90302	28.99	2.2105	2.0583
	2.93	0.88734	29.38	2.5679	2.0226	0.88722	29.39	2.5706	2.0223	0.88708	29.39	2.5738	2.0220	0.88592	29.41	2.6003	2.0193
3	2.96	0.91529	28.06	1.9308	2.0863	0.91514	28.06	1.9342	2.0859	0.91496	28.07	1.9383	2.0855	0.91348	28.10	1.9721	2.0821
	2.95	0.89425	28.59	2.4104	2.0383	0.89412	28.59	2.4134	2.0380	0.89395	28.59	2.4172	2.0376	0.89258	28.62	2.4485	2.0345
	2.94	0.87463	29.09	2.8576	1.9936	0.87449	29.09	2.8608	1.9933	0.87433	29.10	2.8645	1.9929	0.87305	29.12	2.8936	1.9900
	2.93	0.85616	29.58	3.2786	1.9515	0.85604	29.58	3.2814	1.9512	0.85588	29.58	3.2850	1.9508	0.85467	29.61	3.3137	1.9480
4	2.96	0.89703	28.15	2.3470	2.0446	0.89688	28.15	2.3505	2.0443	0.89668	28.15	2.3550	2.0438	0.89515	21.18	2.3899	2.0404
	2.95	0.8749	28.72	2.8515	1.9942	0.87476	28.72	2.8547	1.9939	0.87458	28.73	2.8588	1.9935	0.87316	28.76	2.8911	1.9902
	2.94	0.85447	29.27	3.3172	1.9476	0.85433	29.27	3.3203	1.9473	0.85417	29.27	3.3240	1.9469	0.85284	29.30	3.3543	1.9439
	2.93	0.8354	29.79	3.7518	1.9042	0.83528	29.79	3.7546	1.9039	0.83512	29.80	3.7582	1.9035	0.83388	29.82	3.7865	1.9007
5	2.96	0.88363	28.25	2.6525	2.0141	0.88347	28.25	2.6561	2.0137	0.88328	28.26	2.6605	2.0133	0.8817	28.29	2.6965	2.0097
	2.95	0.8609	28.86	3.1706	1.9623	0.86075	28.86	3.1740	1.9619	0.86057	28.86	3.1781	1.9615	0.85912	28.89	3.2112	1.9582
	2.94	0.84004	29.43	3.6461	1.9147	0.83991	29.43	3.6490	1.9144	0.83974	29.43	3.6529	1.9141	0.83839	29.46	3.6837	1.9110
	2.93	0.82068	29.98	4.0874	1.8706	0.82056	29.98	4.0901	1.8703	0.8204	29.98	4.0937	1.8700	0.81914	30.01	4.1225	1.8671

Table 6. Location, velocity and distance of orbit from both primaries for A_2 = 0.00001, 0.00005, 0.0001, 0.0005 for Sun-Earth system.

No. of loop	C	x	V (km·sec⁻¹)	D₁ (10⁷ km)	D₂ (10⁸ km)	x	V (km·sec⁻¹)	D₁ (10⁷ km)	D₂ (10⁸ km)	x	V (km·sec⁻¹)	D₁ (10⁷ km)	D₂ (10⁸ km)	x	V (km·sec⁻¹)	D₁ (10⁷ km)	D₂ (10⁸ km)
			A_2 = 0.00001				A_2 = 0.00005				A_2 = 0.0001				A_2 = 0.0005		
1	2.96	0.983	35.32	0.2542	1.4705	0.9829	35.32	0.2557	1.4704	0.9828	35.33	0.2572	1.4702	0.9817	35.36	0.2737	1.4686
	2.95	0.9679	35.70	0.4801	1.4479	0.96782	35.70	0.4813	1.4478	0.9677	35.70	0.4831	1.4476	0.9666	35.72	0.4996	1.4460
	2.94	0.95325	36.09	0.6993	1.4260	0.95315	36.09	0.7008	1.4259	0.95304	36.09	0.7024	1.4257	0.952	36.11	0.7180	1.4241
	2.93	0.939	36.47	0.9125	1.4047	0.9389	36.47	0.9140	1.4045	0.93877	36.48	0.9159	1.4044	0.93775	36.50	0.9312	1.4028
2	2.96	0.94155	34.75	0.8743	1.40856	0.9414	34.75	0.8766	1.4083	0.94125	34.75	0.8788	1.4081	0.9399	34.78	0.8990	1.4060
	2.95	0.92255	35.30	1.1586	1.3801	0.92244	35.30	1.1602	1.3799	0.92226	35.30	1.1629	1.3797	0.921	35.33	1.1817	1.3778
	2.94	0.90455	35.83	1.4278	1.3532	0.90442	35.84	1.4298	1.3530	0.90426	35.84	1.4322	1.3527	0.90305	35.87	1.4503	1.3509
	2.93	0.88737	36.36	1.6848	1.3275	0.88725	36.36	1.6866	1.3273	0.8871	36.36	1.6889	1.3271	0.88595	36.39	1.7061	1.3253
3	2.96	0.91535	34.72	1.2663	1.3693	0.9152	34.73	1.2685	1.3691	0.915	34.73	1.2715	1.3688	0.91354	34.77	1.2933	1.3666
	2.95	0.8943	35.37	1.5812	1.3378	0.89416	35.37	1.5833	1.3376	0.894	35.38	1.5857	1.3374	0.89262	35.41	1.6063	1.3353
	2.94	0.87465	35.99	1.8751	1.3084	0.87453	36.00	1.8769	1.3083	0.87438	36.00	1.8792	1.3080	0.87309	36.03	1.8985	1.3061
	2.93	0.8562	36.60	2.1512	1.2808	0.85608	36.60	2.1529	1.2807	0.85592	36.60	2.1553	1.2804	0.8547	36.63	2.1736	1.2786
4	2.96	0.8971	34.83	1.5393	1.34206	0.89695	34.83	1.5415	1.3418	0.89675	34.83	1.5445	1.3415	0.8952	34.87	1.5677	1.3392
	2.95	0.87495	35.54	1.8707	1.3089	0.87482	35.54	1.8726	1.3087	0.87464	35.54	1.8753	1.3084	0.87321	35.58	1.8967	1.3063
	2.94	0.8545	36.21	2.1766	1.2783	0.85438	36.21	2.1784	1.2781	0.85421	36.22	2.1809	1.2779	0.85289	36.25	2.2007	1.2759
	2.93	0.83544	36.86	2.4617	1.2498	0.83532	36.86	2.4635	1.2496	0.83516	36.87	2.4659	1.2494	0.83392	36.90	2.4845	1.2475
5	2.96	0.8837	34.95	1.7398	1.3220	0.88353	34.96	1.7423	1.3217	0.88334	34.96	1.7451	1.3214	0.88175	35.00	1.7689	1.3191
	2.95	0.86095	35.70	2.0801	1.2879	0.8608	35.71	2.0823	1.2877	0.86062	35.71	2.0850	1.2874	0.85918	35.75	2.1066	1.2853
	2.94	0.8401	36.41	2.3920	1.2567	0.83995	36.41	2.3943	1.2565	0.83978	36.42	2.3968	1.2563	0.83844	36.46	2.4168	1.2543
	2.93	0.82072	37.09	2.6819	1.2278	0.8206	37.09	2.6837	1.2276	0.82044	37.10	2.6861	1.2273	0.81918	37.13	2.7050	1.2254

number of loop as A_2 increases initial velocity increases and D_1 increases so, D_2 decreases. So, the effect of Jacobi constant C and oblateness A_2 is opposite in nature. For given value of A_2 and C as number of loops increases, D_1 increases and D_2 decreases where as V decreases up to loops 1 - 3 and then increases from 3 - 5-loop orbits. From **Table 5**, it is observed that single-loop orbit for $A_2 = 0.00001$ is closest to Mars and this distance is 3.886×10^7 km. which is obtained using $C = 2.96$. Similar notations are used in **Table 6** also.

From **Table 6**, it is observed that single-loop orbit for $A_2 = 0.00001$ is closest to Earth and this distance is 2.542×10^7 km. which is obtained using $C = 2.96$. Here D_1 is the distance of secondary body from Earth.

4. Prediction of Orbit through Regression Analysis

The locations of single-loop and two loops periodic orbits obtained for different values of C for Sun-Mars system $A_2 = 0.00001$ from PSS is displayed in **Table 7**. Using regression analysis we have displayed the predicted position of the orbit for different values of C. The predicted and exact values of positions together with error estimates are displayed in **Table 8**. The best fit curve for single-loop is a straight line with equation

Table 7. Variation in location of periodic orbit when $A_2 = 0.00001$ for Sun-Mars system.

Number of loop	C	X
1	2.96	0.98295
	2.95	0.9679
	2.94	0.95324
	2.93	0.93896
2	2.96	0.94149
	2.95	0.92251
	2.94	0.9045
	2.93	0.88734

Table 8. Prediction and error for periodic orbit when $A_2 = 0.00001$ for Sun-Mars system.

Number of loop	C	Predicted	Exact	Error
1	2.92	0.92372	0.92508	0.00136
	2.925	0.93105	0.93198	0.00093
	2.935	0.94571	0.94605	0.00034
	2.945	0.96037	0.9605	0.00013
	2.955	0.97503	0.9754	0.00037
	2.965	0.98969	0.99069	0.001
2	2.92	0.86768	0.87092	0.00324
	2.925	0.8767	0.87904	0.00234
	2.935	0.89474	0.89582	0.00108
	2.945	0.91278	0.9134	0.00062
	2.955	0.93082	0.931875	0.001055
	2.965	0.94886	0.9514	0.00254

$x = 1.466 \times C - 3.357$ and the coefficient of determination $R^2 = 0.999$, whereas, for two-loop periodic orbit regression line is $x = 1.804 \times C - 4.4$ and $R^2 = 0.999$.

Similar calculations are made for one-loop and two loops orbits for $A_2 = 0.0005$ and the relevant estimates are displayed in Table 9 and Table 10.

The regression curve for single-loop periodic orbit is given by
$x = 1.9 \times C^2 - 9.728 \times C + 13.13$ with $R^2 = 1$ and for two-loops periodic orbit regression curve is $x = 4.475 \times C^2 - 24.56 \times C + 34.43$ with $R^2 = 1$.

It can be observed that as C increases the error between the predicted and exact values of the position of periodic orbits increases. The PSS together with regression analysis will help one to locate the position of the periodic orbit with less effort, using the predicted positions from the analysis.

The variation of position x with oblateness A_2 for Sun-Mars system for fixed value of $C = 2.96$ using PSS is shown in Table 11. The predicted and exact values of the position of orbits together with error estimates using regression analysis are shown in Table 12. For single-loop the best fit regression curve is $x = -500.7 \times A_2^2 - 2.5 \times A_2 + 0.983$ with $R^2 = 1$, where as for two loops orbit $x = -39.14 \times A_2^2 - 3.329 \times A_2 + 0.941$ with $R^2 = 1$.

Table 9. Variation in location of periodic orbit when $A_2 = 0.0005$ for Sun-Mars system.

Number of loop	C	X
1	2.96	0.9816
	2.95	0.9666
	2.94	0.95196
	2.93	0.93772
2	2.96	0.93985
	2.95	0.92096
	2.94	0.90302
	2.93	0.88592

Table 10. Prediction and error for periodic orbit when $A_2 = 0.0005$ for Sun-Mars system.

Number of loop	C	Predicted	Exact	Error
1	2.92	0.9244	0.92387	−0.00053
	2.925	0.931288	0.93075	−0.00054
	2.935	0.945348	0.9448	−0.00055
	2.945	0.959787	0.95922	−0.00057
	2.955	0.974607	0.97404	−0.00057
	2.965	0.989808	0.98929	−0.00052
2	2.92	0.87044	0.86955	−0.00089
	2.925	0.878422	0.87904	0.000618
	2.935	0.895057	0.89582	0.000763
	2.945	0.912587	0.9134	0.000813
	2.955	0.931012	0.931875	0.000863
	2.965	0.950332	0.9514	0.001068

The variation of position x for different values of C for one-loop and two loops orbit for $A_2 = 0.00001$ for Sun-Earth system is shown in **Table 13**.

Using regression analysis we have displayed predicted and exact values of position together with error estimates are shown in **Table 14**. As in the case of Sun-Mars system the error estimates decreases, with increase in C for both single-loop and two-loops orbits. The best fit curve for single-loop orbit is given by $x = 1.466 \times C - 3.358$ with $R^2 = 0.999$, and for two loops orbit regression line $x = 1.805 \times C - 4.402$ with $R^2 = 0.999$.

Similar estimates are displayed for $A_2 = 0.00005$ in **Table 15** and **Table 16**, for Sun-Earth system.

For single-loop orbit regression curve is given by $x = 2.125 \times C^2 - 11.05 \times C + 15.07$

Table 11. Variation in location of periodic orbit when $C = 2.96$ for Sun-Mars system.

Number of loop	A_2	X
1	0.00001	0.98295
	0.00005	0.98285
	0.0001	0.98272
	0.0005	0.9816
2	0.00001	0.94149
	0.00005	0.94136
	0.0001	0.94119
	0.0005	0.93985

Table 12. Prediction and error for periodic orbit when $C = 2.96$ for Sun-Mars system.

Number of loop	A_2	Predicted	Exact	Error
1	0.000025	0.982937187	0.98293	−7.187E−06
	0.000075	0.982809684	0.9828	−9.683E−06
	0.00025	0.982343706	0.98233	−1.3706E−05
	0.00075	0.980843356	0.98095	0.000106644
2	0.000025	0.940916751	0.94145	0.000533249
	0.000075	0.940750105	0.94128	0.000529895
	0.00025	0.940165304	0.94069	0.000524696
	0.00075	0.938481234	0.93902	0.000538766

Table 13. Variation in location of periodic orbit when $A_2 = 0.00001$ for Sun-Earth system.

Number of loop	C	X
1	2.96	0.983
	2.95	0.9679
	2.94	0.95325
	2.93	0.939
2	2.96	0.94155
	2.95	0.92255
	2.94	0.90455
	2.93	0.88737

Table 14. Prediction and error for periodic orbit when $A_2 = 0.00001$ for Sun-Earth system.

Number of loop	C	Predicted	Exact	Error
1	2.92	0.92272	0.9251	0.00238
	2.925	0.93005	0.932	0.00195
	2.935	0.94471	0.9461	0.00139
	2.945	0.95937	0.96055	0.00118
	2.955	0.97403	0.97542	0.00139
	2.965	0.98869	0.99072	0.00203
2	2.92	0.8686	0.87095	0.00235
	2.925	0.877625	0.87909	0.001465
	2.935	0.895675	0.89588	0.000205
	2.945	0.913725	0.91342	−0.0003
	2.955	0.931775	0.9319	0.000125
	2.965	0.949825	0.95147	0.001645

Table 15. Variation in location of periodic orbit when $A_2 = 0.00005$ for Sun-Earth system.

Number of loop	C	X
1	2.96	0.9817
	2.95	0.9666
	2.94	0.952
	2.93	0.93775
2	2.96	0.9414
	2.95	0.92244
	2.94	0.90442
	2.93	0.88725

Table 16. Prediction and error for periodic orbit when $A_2 = 0.00005$ for Sun-Earth system.

Number of loop	C	Predicted	Exact	Error
1	2.92	0.9226	0.92501	0.00241
	2.925	0.929453	0.93189	0.002437
	2.935	0.943478	0.94599	0.002512
	2.945	0.957928	0.96044	0.002512
	2.955	0.972803	0.97532	0.002517
	2.965	0.988103	0.99062	0.002517
2	2.92	0.87964	0.87083	−0.00881
	2.925	0.887672	0.87896	−0.00871
	2.935	0.904407	0.89573	−0.00868
	2.945	0.922037	0.91333	−0.00871
	2.955	0.940562	0.9318	−0.00876
	2.965	0.959982	0.9513	−0.00868

with $R^2 = 1$ and for two-loops orbit regression curve is given by

$$x = 4.475 \times C^2 - 24.55 \times C + 34.41 \quad \text{with } R^2 = 1.$$

The variation of position x with oblateness A_2 for Sun-Earth system is shown in **Table 17** for a fix value of $C = 2.96$.

The predicted and exact value of position together with error estimates are shown in **Table 18**.

The equation of the best fit curve for single-loop is

$x = -1056 \times A_2^2 - 2.105 \times A_2 + 0.983$ with $R^2 = 1$, where as for two-loops orbit regression curve is $x = -58.59 \times A_2^2 - 3.325 \times A_2 + 0.941$ with $R^2 = 1$.

5. Conclusions

In this paper, we have studied the effect of oblateness on the position, shape and size of closed periodic orbit with loops varying from 1 to 5 for Sun-Mars and Sun-Earth systems, respectively. It is concluded that for given number of loops and given C, as oblateness increases, location of periodic orbit moves towards Sun. For given C and given oblateness, as number of loops increases, location of periodic orbits shifts towards Sun. Also, for given value of oblateness and given number of loops, as C decreases, location of periodic orbit moves towards Sun. Also, period of the orbit increases as number of loops increases. It is also observed that single-loop orbit is closest to second primary body. Further, as number of loops decreases, width of the orbit increases. The distance of closest approach of the infinitesimal particle from the smaller primary increases with oblateness and number of loops for a given C. Thus, the present analysis of the two systems—Sun-Mars and Sun-Earth systems—using PSS technique reveals that A_2 and C has

Table 17. Variation in location of periodic orbit when $C = 2.96$ for Sun-Earth system.

Number of loop	A_2	X
	0.00001	0.983
	0.00005	0.9829
1	0.0001	0.9828
	0.0005	0.9817
	0.00001	0.94155
	0.00005	0.9414
2	0.0001	0.94125
	0.0005	0.9399

Table 18. Prediction and error for periodic orbit when $C = 2.96$ for Sun-Earth system.

Number of loop	A_2	Predicted	Exact	Error
	0.000025	0.982946715	0.98294	−6.715E−06
	0.000075	0.982836185	0.98283	−6.185E−06
1	0.00025	0.98240775	0.9824	−7.75E−06
	0.00075	0.98082725	0.981	0.00017275
	0.000025	0.940916838	0.9415	0.000583162
	0.000075	0.940750295	0.94133	0.000579705
2	0.00025	0.940165088	0.94074	0.000574912
	0.00075	0.938473293	0.93906	0.000586707

substantial effect on the position, shape and size of the obit. The PSS together with regression analysis will help one to locate the position of the periodic orbit with less effort, using the predicted positions from the analysis.

It can be observed that for given oblateness and given number of loops, as Jacobi constant decreases, initial velocity of infinitesimal particle (spacecraft) and distance of spacecraft from second primary increase and distance of spacecraft from first primary body decreases. For given Jacobi constant and given number of loops, as oblateness increases, initial velocity increases and distance of spacecraft from second primary increases. So, distance of spacecraft from first primary decreases. Thus, the effect of Jacobi constant C and oblateness coefficient A_2 is opposite in nature. For given value of oblateness coefficient and Jacobi constant, as number of loops increases, distance of spacecraft from second primary increases and distance of spacecraft from first primary decreases where as initial velocity of spacecraft decreases up to loops 1 - 3 and then increases from 3 - 5. It is further observed that for Sun-Mars system, single-loop orbit for $A_2 = 0.00001$ and $C = 2.96$ is closest to Mars and this distance is 3.886×10^7 km. Whereas for Sun-Earth system, single-loop orbit for $A_2 = 0.00001$ and $C = 2.96$ is closest to Earth and this distance is 2.542×10^7 km. Since stability of this class of periodic orbits is very low, it can be used for designing low-energy trajectory design for space mission.

Acknowledgements

References

[1] Koon, W.S., Lo, M.W., Marsden, J.E. and Ross, S. (2001) Low Energy Transfer to the Moon. Celestial Mechanics and Dynamical Astronomy. *Celestial Mechanics and Dynamical Astronomy*, **81**, 63-73. https://doi.org/10.1023/A:1013359120468

[2] Koon, W.S., Lo, M.W., Marsden, J.E. and Ross, S. (2011) Dynamical Systems, the Three-Body Problem and Space Mission Design. http://www.cds.caltech.edu/~marsden/books/Mission_Design.html

[3] Szebehely, V. (1967) Theory of Orbits. Academic Press, San Diego.

[4] Murray, C.D. and Dermot, S.F. (1999) Solar System Dynamics. Cambridge University Press, Cambridge.

[5] Dutt, P. and Sharma, R.K. (2010) Analysis of Periodic and Quasi-Periodic Orbits in the Earth-Moon System. *Journal of Guidance, Control, and Dynamics,* **33**, 1010-1017. https://doi.org/10.2514/1.46400

[6] Dutt, P. and Sharma, R.K. (2011) Evolution of Periodic Orbits in the Sun-Mars System. *Journal of Guidance, Control, and Dynamics,* **34**, 635-644. https://doi.org/10.2514/1.51101

[7] Safiyabeevi, A. and Sharma, R.K. (2011) Oblateness Effect of Saturn on Periodic Orbits in the Saturn-Titan Restricted Three-Body Problem. *Astrophysics and Space Science*, **340**, 245-261. https://doi.org/10.1007/s10509-012-1052-3

[8] Dutt, P. and Sharma, R.K. (2012) On the Evolution of the "f" Family in the Restricted Three-Body Problem. *Astrophysics and Space Science*, **340**, 63-70. https://doi.org/10.1007/s10509-012-1039-0

[9] Tsirogiannis, G.A. and Douskos, C.N. and Perdios, E.A. (2006) Computation of the Liapunov Orbits in the Photogravitational RTBP with Oblateness. *Astrophysics and Space Science*, **305**, 389-398. https://doi.org/10.1007/s10509-006-9171-3

[10] Perdiou, A.E., Perdios, E.A. and Kalantonis, V.S. (2012) Periodic Orbits of the Hill Problem with Radiation and Oblateness. *Astrophysics and Space Science*, **342**, 19-30. https://doi.org/10.1007/s10509-012-1145-z

[11] Elshaboury, S.M., Abouelmagd, E.I., Kalantonis, V.S. and Perdios, E.A. (2016) The Planar Restricted Three-Body Problem When Both Primaries Are Triaxial Rigid Bodies: Equilibrium Points and Periodic Orbits. *Astrophysics and Space Science*, **361**, 315. https://doi.org/10.1007/s10509-016-2894-x

[12] Mittal, A., Ahmad, I. and Bhatnagar, K.B. (2009) Periodic Orbits Generated by Lagrangian Solutions of the Restricted Three Body Problem When One of the Primaries Is an Oblate Body. *Astrophysics and Space Science*, **319**, 63-73. https://doi.org/10.1007/s10509-008-9942-0

[13] Mittal, A., Ahmad, I. and Bhatnagar, K.B. (2009) Periodic Orbits in the Photogravitational Restricted Problem with the Smaller Primary an Oblate Body. *Astrophysics and Space Science*, **323**, 65-73. https://doi.org/10.1007/s10509-009-0038-2

[14] Perdios, E.A. and Kalantonis, V.S. (2006) Computation of the Liapunov Orbits in the Photogravitational RTBP with Oblateness. *Astrophysics and Space Science*, **305**, 389-398. https://doi.org/10.1007/s10509-006-9171-3

[15] Broucke, R.A. (1968) Technical Report. Vol. 32, Jet Propulsion Lab., Pasadena.

[16] Jefferys, W.H. (1971) An Atlas of Surfaces of Section for the Restricted Problem of Three Bodies. Published at the Department of Astronomy of the University of Texas at Austin, Ser. II, 3, 6.

[17] Smith, R.H. (1991) The Onset of Chaotic Motion in the Restricted Problem of Three Bodies. PhD Thesis, University of Texas at Austin, Austin.

[18] Contopoulos, G. (1991) Periodic Orbits and Chaos around Two Fixed Black Holes. *Proceedings of the Royal Society of London*, **435**, 551-562.

[19] Poincare, H. (1892) Celeste. Vol. 1, Gauthier-Villas, Paris, 82.

[20] Winter, O.C. and Murray, C.D. (1994) QMW Notes No. 16. Queen Marry and Westfield College, London.

[21] Winter, O.C. and Murray, C.D. (1994) QMW Notes No. 17. Queen Marry and Westfield College, London.

[22] Winter, O.C. and Murray, C.D. (1997) Resonance and Chaos. *Astronomy & Astrophysics*, **319**, 290-304.

[23] Winter, O.C. and Murray, C.D. (1997) Resonance and Chaos. II. Exterior Resonances and Asymmetric Libration. *Astronomy & Astrophysics*, **328**, 399-408.

[24] Pathak, N., Sharma, R.K. and Thomas, V.O. (2016) Evolution of Periodic Orbits in the Sun-Saturn System. *International Journal of Astronomy and Astrophysics*, **6**, 175-197. https://doi.org/10.4236/ijaa.2016.62015

[25] Pathak. N. and Thomas, V.O. (2016) Evolution of the "f" Family Orbits in the Photo Gravitational Sun-Saturn System with Oblateness. *International Journal of Astronomy and Astrophysics*, **9**, 254-271.

[26] Stromgren, E. (1935) O. Connaissance Actualle des Orbites dans le Problem des Trois Corps. vol. 9, Publications and Minor Communications of Copenhagen Observatory, Publication 100, Copenhagen University, Astronomical Observatory, Denmark.

[27] Sharma, R.K. (1987) The Linear Stability of Libration Points of the Photogravitational Restricted Three-Body Problem When the Smaller Primary Is an Oblate Spheroid. *Astrophysics and Space Science*, **135**, 271-281. https://doi.org/10.1007/BF00641562